NASA TECHNICAL MEMORANDUM

NASA TM X-72816

(NASA-TM-X-72816) RESIZING PROCEDURE FOR OPTIMUM DESIGN OF STRUCTURES UNDER COMBINED MECHANICAL AND THERMAL LOADING (NASA) 25 p HC $3.50 CSCL 13M

N76-18530

Unclas
G3/39 18450

NASA TM X-72816

RESIZING PROCEDURE FOR OPTIMUM DESIGN OF STRUCTURES UNDER COMBINED MECHANICAL AND THERMAL LOADING

Howard M. Adelman
and
R. Narayanaswami

JANUARY 1976

This informal documentation medium is used to provide accelerated or special release of technical information to selected users. The contents may not meet NASA formal editing and publication standards, may be revised, or may be incorporated in another publication.

NATIONAL AERONAUTICS AND SPACE ADMINISTRATION
LANGLEY RESEARCH CENTER, HAMPTON, VIRGINIA 23665

1. Report No.	2. Government Accession No.	3. Recipient's Catalog No.
NASA TM X-72816		
4. Title and Subtitle Resizing Procedure for Optimum Design of Structures Under Combined Mechanical and Thermal Loading		5. Report Date January 1976 6. Performing Organization Code
7. Author(s) Howard M. Adelman and R. Narayanaswami		8. Performing Organization Report No. 10. Work Unit No. 743-01-11-03
9. Performing Organization Name and Address NASA Langley Research Center Hampton, VA 23665		11. Contract or Grant No. 13. Type of Report and Period Covered Technical Memorandum
12. Sponsoring Agency Name and Address National Aeronautics and Space Administration Washington, DC 20546		14. Sponsoring Agency Code
15. Supplementary Notes		

16. Abstract

This paper describes an algorithm for resizing structures subjected to combined thermal and mechanical loading. The algorithm is applicable to uniaxial stress elements (rods) and membrane biaxial stress members. The procedure, called thermal fully-stressed design (TFSD) is based on the basic difference between mechanical and thermal stresses in their response to resizing. Namely, the mechanical stresses are more sensitive to structure resizing than are the thermal stresses. As a result, the TFSD technique is found to converge in fewer iterations than ordinary fully-stressed design (FSD) for problems where thermal stresses are comparable to the mechanical stresses.

The improved convergence is demonstrated by example with a study of a simplified wing structure, built-up with rods and membranes and subjected to a combination of mechanical loads and a three-dimensional temperature distribution. Both the FSD and TFSD methods converged to the same final design and TFSD required far fewer iterations to converge than did FSD.

17. Key Words (Suggested by Author(s))	18. Distribution Statement		
Optimum Design Thermal Stress Fully Stressed Design	Unclassified - Unlimited Subject Category 39		
19. Security Classif. (of this report)	20. Security Classif. (of this page)	21. No. of Pages	22. Price*
Unclassified	Unclassified	24	$3.25

RESIZING PROCEDURE FOR OPTIMUM DESIGN OF STRUCTURES UNDER COMBINED MECHANICAL AND THERMAL LOADING

By Howard M. Adelman and R. Narayanaswami
Langley Research Center

SUMMARY

This paper describes an algorithm for resizing structures subjected to combined thermal and mechanical loading. The algorithm is applicable to uniaxial stress elements (rods) and membrane biaxial stress members. The procedure, called thermal fully-stressed design (TFSD) is based on the basic difference between mechanical and thermal stresses in their response to resizing. Namely, the mechanical stresses are more sensitive to structure resizing than are the thermal stresses. As a result, the TFSD technique is found to converge in fewer iterations than ordinary fully-stressed design (FSD) for problems where thermal stresses are comparable to the mechanical stresses.

The improved convergence is demonstrated by example with a study of a simplified wing structure, built-up with rods and membranes and subjected to a combination of mechanical loads and a three-dimensional temperature distribution. Both the FSD and TFSD methods converged to the same final design and TFSD required far fewer iterations to converge than did FSD.

INTRODUCTION

Probably the most widely used approach for sizing of flight structures under strength and minimum gage constraints is fully-stressed design (FSD). In this method the structural sizes are iterated with the step size depending on the ratio of the total stress to the allowable stress (refs. 1-3). The FSD procedure is traditionally used to obtain, at a reasonable computational cost, designs which if not at a minimum weight are at least acceptably close to the minimum weight (ref. 2).

Almost all of the experience with FSD has been with structures primarily under mechanical loading as opposed to thermal loading. The temptation in including thermal loads in FSD is to simply continue to use the total stresses in computing the iteration step size. This approach seems satisfactory when mechanical stresses dominate the thermal stresses (ref. 4). Convergence may be slow, however, when thermal stresses are comparable to mechanical stresses. The slower convergence is associated with relative insensitivity of the thermal stresses to changes in structural sizing. Procedures are therefore needed which take into account the differing responses of thermal and mechanical stresses to changes in structural sizes.

An improved variant of FSD was described in reference 4 for uniaxial stress members. It was demonstrated for automated sizing of truss-type structures. For problems having substantial thermal stress, the new procedure (called thermal fully-stressed design or TFSD) was found to converge in far fewer iterations than ordinary FSD. This paper extends the TFSD procedure to biaxial stress members using the Von Mises failure criterion. The TFSD resizing procedure for uniaxial stress members is restated, the new procedure for biaxial stress members is developed, and results are given from an application of the procedure to size a simplified wing structure.

LIST OF SYMBOLS

A	cross sectional area of a bar
b	thermal-mechanical stress coupling term (eqn 8)
E	Young's modulus
N_{FSD}	number of iterations required for FSD to converge to within 5 percent of final mass
N_{TFSD}	number of iterations required for TFSD to converge to within 5 percent of final mass
r	$= t_{i+1}/t_i$
t	thickness of a membrane
V	$= \left[\sigma_x^2 + \sigma_y^2 - \sigma_x\sigma_y + 3\sigma_{xy}^2\right]^{1/2}$, Von Mises stress measure
α	coefficient of linear thermal expansion
ρ	weight density
ν	Poisson's ratio
σ	stress component

Subscripts

a	allowable
i	iteration number
M	mechanical
T	thermal
x, y	orthogonal coordinate directions in plane of membrane element

THE TFSD ALGORITHM FOR UNIAXIAL STRESS MEMBERS

The TFSD resizing algorithm for uniaxial stress members (rods) is given in reference 4 as

$$A_{i+1} = \frac{\sigma_{Mi}}{\sigma_{a,M} - \sigma_{Ti}} A_i \tag{1}$$

In equation (1) σ_M is the stress due to mechanical loads acting alone, σ_T is the stress due to thermal loads acting alone and $\sigma_{a,\,M}$ is either the tensile or compressive allowable stress, depending on the sign of σ_M. The algorithm of equation (1) drives each element toward the condition

$$\frac{\sigma_M}{\sigma_{a,M} - \sigma_T} = 1 \tag{2}$$

Thus, the mechanical stress is driven toward an effective allowable stress given by the algebraic difference between the material allowable stress and thermal stress. For later reference, the usual FSD algorithm is given by

$$A_{i+1} = \frac{\sigma_{Mi} + \sigma_{Ti}}{\sigma_a} A_i \tag{3}$$

where in equation (3), σ_a is either the tensile or compressive allowable stress, depending on the sign of the total stress as given by the numerator. The algorithm in equation (3) drives each element toward the condition

$$\frac{\sigma_M + \sigma_T}{\sigma_a} = 1$$

DEVELOPMENT OF TFSD RESIZING ALGORITHM FOR BIAXIAL STRESS MEMBERS

The Von Mises failure criterion for isotropic biaxial stress members is

$$V\left(\sigma_x,\sigma_y,\sigma_{xy}\right) \equiv \left[\sigma_x^2 + \sigma_y^2 - \sigma_x\,\sigma_y + 3\sigma_{xy}^2\right]^{1/2} = \sigma_a \tag{4}$$

where σ_x and σ_y are direct stresses along orthogonal coordinate directions in the plane of the element, σ_{xy} is the shear stress on that plane and σ_a is the allowable stress. In preparation for generalizing the resizing formula from uniaxial to biaxial stress members, rearrange equation (1) as follows:

$$\frac{\sigma_{Mi}}{A_{i+1}/A_i} + \sigma_{Ti} = \sigma_{a,M} \tag{5}$$

By analogy, the corresponding statement for biaxially stressed members is

$$V\left(\frac{\sigma_{xMi}}{r_i} + \sigma_{xTi},\ \frac{\sigma_{yMi}}{r_i} + \sigma_{yTi},\ \frac{\sigma_{xyMi}}{r_i} + \sigma_{xyTi}\right) = \sigma_a \tag{6}$$

where $r_i = t_{i+1}/t_i$ and t is the element thickness. Expansion of equation (6) using equation (4) gives

$$\left(V_{T,i}^2 - \sigma_a^2\right) r_i^2 + b_i r_i + V_{M,i}^2 = 0 \tag{7}$$

where

$$\left.\begin{aligned}
V_T^2 &= \sigma_{xT}^2 + \sigma_{yT}^2 - \sigma_{xT}\sigma_{yT} + 3\sigma_{xyT}^2 \\
V_M^2 &= \sigma_{xM}^2 + \sigma_{yM}^2 - \sigma_{xM}\sigma_{yM} + 3\sigma_{xyM}^2 \\
b &= 2\sigma_{xT}\sigma_{xM} + 2\sigma_{yT}\sigma_{yM} - \sigma_{xT}\sigma_{yM} \\
&\quad - \sigma_{yT}\sigma_{xM} + 6\sigma_{xyT}\sigma_{xyM}
\end{aligned}\right\} \tag{8}$$

Solution of equation (7) by the quadratic formula gives the resizing algorithm

$$t_{i+1} = \left[\frac{b_i}{2\left(\sigma_a^2 - V_{Ti}^2\right)} \pm \sqrt{\frac{b_i^2}{4\left(\sigma_a^2 - V_{Ti}^2\right)^2} + \frac{V_{Mi}^2}{\sigma_a^2 - V_{Ti}^2}} \right] t_i \tag{9}$$

The choice of sign in front of the radical is dictated by the requirement that the bracketed quantity be positive since only positive thicknesses are physically meaningful. When $V_T < \sigma_a$ the positive sign must be chosen. When $V_T > \sigma_a$ and $b > 0$ the algorithm is inapplicable since no acceptable design exists without thermal stress reduction by non-structural means. When $V_T > \sigma_a$ and $b < 0$, either the positive or negative sign may be used provided the radicand is positive. In the later case intuition would suggest the choice of the negative sign since the minimum weight design is sought. The authors' use of the algorithm has been limited to cases wherein $V_T < \sigma_a$ and hence the positive sign was used exclusively in equation (9).

For later reference, the corresponding FSD resizing algorithm used to compare results with TFSD is

$$t_{i+1} = \frac{V_i}{\sigma_a} t_i \tag{10}$$

where V is defined by equation (4).

APPLICATION TO A BUILT-UP WING

To illustrate the application of the TFSD resizing algorithm and to compare the algorithm with ordinary FSD, calculations were carried out using a computer program incorporating both the TFSD and the FSD procedures. Finite element methods using standard rod elements and the "TRIM 6" (ref. 5) triangular membrane elements were used for the analyses.

The structure used in the calculations is a simplified low-aspect ratio built-up wing structure (shown in fig. 1) which is roughly based on the configuration studied extensively in reference 6. The ribs and spars are modeled by trusses with a total of 85 rod elements. The upper and lower skins are each modeled by 5 membrane elements. As a result there are a total of 95 design variables in the problem including rod areas and membrane thicknesses and the finite element model has 36 grid points. The finite element model is described in Table 1 where grid point coordinates are listed and in Table 2 which gives the connection grid points of each rod element. The loads on the wing consist of concentrated forces representing pressure loads of 13.8 KPa (2 psi) in the positive Z - direction at points on the lower surface in addition to elevon loads and a three-dimensional temperature distribution in which temperatures range up to about 600 K. The loads are tabulated in Table 3 and the temperature distribution is shown in figure 2.

Identical results were obtained for the final design by the TFSD procedure (equations (1) and (9)) and by the FSD procedure (equations (3) and (10)). The final design for the rod areas and membrane thicknesses are given in Tables 4 and 5, respectively. As an aid in interpreting the final design, a pictorial representation of the distribution of membrane thickness is shown in figure 3. The largest thicknesses on both the upper and lower surfaces are in the regions of the trailing edge of the wing, namely elements 4 and 5 on the upper surface and elements 9 and 10 on the lower surface. In these regions, the in-plane mechanical loads are maximum due to the presence of the elevon loads, while the thermal loads which relieve the mechanical loads are smallest. As a result, the largest total stresses occur in membranes 4, 5, 9, and 10.

The important observation from this calculation is made by comparing the number of design iterations required to converge from an arbitrary trial design in which all design variables had unit values. The FSD algorithm required 18 iterations to converge to within 5 percent of the mass of the final design whereas the TFSD obtained this degree of convergence in a single iteration. This type of performance by the TFSD procedure relative to FSD is consistent with previous experience comparing the two methods. In reference 4, TFSD required one-fourth as many iterations as FSD to converge for a structure modeled by rod elements only.

To further investigate the convergence of TFSD relative to FSD, three additional sets of calculations were performed; this time with lower temperature levels but with the same mechanical loads as in Table 3. The TFSD procedure required only a single iteration to converge to within 5 percent of the final mass for all cases. A summary of the convergence of TFSD relative to FSD is shown in Table 6 and figure 4 as a function of T/T_{ref} where T_{ref} represents the highest level of thermal loads and corresponds to the temperatures in figure 2 and Table 3. In the first of these cases, the temperatures were input as 75 percent of those in Table 3 ($T/T_{ref} = .75$). The design for this case is given in Tables 7 and 8 and is 6 percent lighter than the design for the reference temperatures. The FSD algorithm required 10 iterations to converge to within 5 percent of the final mass. In the second case the temperatures were 50 percent of those in Table 3. The final design is given in Tables 9 and 10 and is 9 percent lighter than the design corresponding to the reference temperatures. FSD required 5 iterations to converge within 5 percent of the final mass. In the third case, the temperatures were 25 percent of those in Table 3. The final design given in Tables 11 and 12 is 10 percent lighter than the design for the reference temperatures and FSD required 4 iterations to converge to within 5 percent of final mass.

Table 6. - Effect of Temperature on Relative Efficiency of FSD and TFSD for Sample Problem

T/T_{ref}	0.	.25	.50	.75	1.0
N_{FSD}	1	4	5	10	18
N_{TFSD}	1	1	1	1	1

For this example as well as for the examples of reference 4, thermal stresses are quite insensitive to structural sizing. The superiority of TFSD for these examples is associated with this insensitivity. This will be clear if we imagine a case where thermal stresses are completely independent of structural size in which case TFSD would obviously be superior. It seems reasonable that a broad range of structures will exhibit relative insensitivity of thermal stresses to sizing. Consequently, the TFSD procedure should be widely useful for structures under combined thermal and mechanical loads.

CONCLUDING REMARKS

The paper presents an improved algorithm for resizing structures subjected to combined thermal and mechanical loading. The algorithm originally developed for resizing uniaxial stress elements (rods) is herein extended to biaxial stress elements such as membranes. The algorithm is based on monitoring the mechanical and thermal stresses separately and altering the mechanical stresses rather than the total stresses. The thermal stresses enter into the algorithm by adding to or subtracting from the allowable stresses. The improved algorithm, called thermal fully-stressed design (TFSD) takes account of the basic difference between mechanical and thermal stresses in their response to resizing. Namely, the mechanical stresses are more sensitive to structure resizing than are the thermal stresses. As a result, the TFSD technique tends to converge in fewer iterations than does ordinary fully-stressed design (FSD) for problems where thermal stresses are comparable to the mechanical stresses.

This behavior is demonstrated in the paper by calculations on a simplified built-up wing under a combination of mechanical loads and a three-dimensional temperature distribution. Both the FSD and the TFSD methods converged to the same final design, but TFSD converged much more rapidly than did FSD. Further, the relative efficiency of TFSD relative to FSD increased according to the level of the applied thermal loading.

REFERENCES

1. Giles, Gary L.; Blackburn, Charles L.; and Dixon, Sidney C.: Automated Procedures for Sizing Aerospace Vehicle Structures (SAVES). J. Aircraft, Vol. 9, No. 12, Dec. 1972, pp. 812-819.

2. Lansing, W.; Dwyer, W.; Emerton, R.; and Renalli, E.: Application of Fully-stressed Design Procedures to Wing and Empennage Structures. J. Aircraft, Vol. 8, No. 9, Sept. 1971, pp. 683-688.

3. Gellatly, R. A.; Gallagher, R. H.; and Luberacki, W. A.: Development of a Procedure for Automated Synthesis of Minimum Weight Structures. FDL-TDR-64-141, U. S. Air Force, Oct. 1964. (Available from DDC as AD 611 310).

4. Adelman, Howard M.; Walsh, Joanne L.; and Narayanaswami, R.: An Improved Method for Optimum Design of Mechanically and Thermally Loaded Structures. NASA TN D-7965, 1975.

5. Argyris, J. H.: "Triangular Elements with Linearly Varying Strain for the Matrix Displacement Method", Journal of the Royal Aeronautical Society, Vol. 69, Oct. 1965.

6. Robinson, James C.; McWithey, Robert R.; and Klich, George F.: An Analytic Study of Radiatively Cooled Delta-Wing Structures for Hypersonic Aircraft. NASA TN D-6138, 1971.

TABLE I. - COORDINATES OF GRIDPOINTS
OF WING FINITE ELEMENT MODEL

GRID POINT	X		Y		Z	
	cm	in	cm	in	cm	in
1	0	0	0	0	30.48	12
2	0	0	0	0	0	0
3	190.5	75	0	0	30.48	12
4		75	- 50.8	-20	30.48	12
5		75	0	0	0	0
6		75	- 50.8	-20	0	0
7	381.0	150	0	0	30.48	12
8		150	- 50.8	-20	30.48	12
9		150	-101.6	-40	30.48	12
10		150	0	0	0	0
11		150	- 50.8	-20	0	0
12		150	-101.6	-40	0	0
13	571.5	225	0	0	30.48	12
14		225	-101.6	-40	30.48	12
15		225	-152.4	-60	30.48	12
16		225	0	0	0	0
17		225	-101.6	-40	0	0
18		225	-152.4	-60	0	0
19	762.0	300	0	0	30.48	12
20		300	-101.6	-40	30.48	12
21		300	-203.2	-80	30.48	12
22		300	0	0	0	0
23		300	-101.6	-40	0	0
24		300	-203.2	-80	0	0
25	825.5	325	0	0	30.48	12
26		325	-101.6	-40	30.48	12
27		325	-203.2	-80	30.48	12
28		325	0	0	0	0
29		325	-101.6	-40	0	0
30		325	-203.2	-80	0	0
31	889.0	350	0	0	30.48	12
32		350	-101.6	-40	30.48	12
33		350	-203.2	-80	30.48	12
34		350	0	0	0	0
35		350	-101.6	-40	0	0
36		350	-203.6	-80	0	0

TABLE 2. - CONNECTIVITY TABLE FOR TRUSS ELEMENTS OF WING

Bar	Grid points		Bar	Grid points		Bar	Grid points	
1	1	2	30	3	4	59	9	15
2	3	5	31	8	9	60	13	19
3	4	6	32	7	8	61	14	20
4	7	10	33	14	15	62	15	21
5	8	11	34	13	14	63	19	25
6	9	12	35	20	21	64	20	26
7	13	16	36	19	20	65	21	27
8	14	17	37	26	27	66	25	31
9	15	18	38	25	26	67	26	32
10	19	22	39	32	33	68	27	33
11	20	23	40	31	32	69	2	5
12	21	24	41	5	6	70	2	6
13	25	28	42	11	12	71	5	10
14	26	29	43	10	11	72	6	11
15	27	30	44	17	18	73	6	12
16	31	34	45	16	17	74	10	16
17	32	35	46	23	24	75	12	17
18	33	36	47	22	23	76	12	18
19	3	6	48	29	30	77	16	22
20	8	12	49	28	29	78	17	23
21	7	11	50	35	36	79	18	24
22	14	18	51	34	35	80	22	28
23	13	17	52	1	3	81	23	29
24	20	24	53	1	4	82	24	30
25	19	23	54	3	7	83	28	34
26	26	30	55	4	8	84	29	35
27	25	29	56	4	9	85	30	36
28	32	36	57	7	13			
29	31	35	58	9	14			

TABLE 3. - LOADS AND GRID POINT TEMPERATURES

Grid Point	P_x		P_z		T	
	N	lb	N	lb	K	°F
1					500	440
2			2 224	500	500	440
3					489	420
4					500	440
5			6 672	1500	567	560
6			6 672	1500	500	440
7					483	410
8					489	420
9					500	440
10			8 896	2000	584	590
11			13 344	3000	567	560
12			4 448	1000	500	440
13					472	390
14					489	420
15					500	440
16			13 344	3000	572	570
17			20 017	4500	584	590
18			6 672	1500	500	440
19					456	360
20					483	410
21					500	440
22			5 929	1333	567	560
23			17 793	4000	578	580
24			9 635	2166	500	440
25					444	340
26					478	400
27					500	440
28			4 448	1000	567	560
29			8 896	2000	578	580
30			4 448	1000	500	440
31					433	320
32	183 490	41 250			472	390
33	183 490	41 250			500	440
34			2 962	666	567	560
35	-183 490	-41 250	4 448	1000	572	570
36	-183 490	-41 250	1 482	333	500	440

TABLE 4. - FINAL DESIGN OF TRUSS ELEMENTS OBTAINED BY TFSD AND FSD

Temperatures and Loads Given in Table 3.

Bar	Area cm^2	Area in^2	Bar	Area cm^2	Area in^2	Bar	Area cm^2	Area in^2
1	.0064	.001	30	.0064	.001	59	.0064	.001
2			31			60		
3			32			61		
4			33			62	.2668	.04136
5	.04543	.007042	34			63	.0064	.001
6	.0064	.001	35			64		
7	.0064	.001	36			65		
8	.06813	.01056	37			66		
9	.0064	.001	38			67		
10	.0064	.001	39			68	.5319	.08244
11	.09845	.01526	40	1.394	.2160	69	.0064	.001
12	.0064	.001	41	.0064	.001	70		
13	.0064	.001	42			71		
14	.04543	.007042	43			72		
15	.0064	.001	44			73		
16	.0064	.001	45			74		
17	.01514	.002347	46			75		
18	.0064	.001	47			76		
19	.13245	.02053	48			77		
20	.08832	.01369	49			78		
21	.3532	.05475	50			79		
22	.1324	.02053	51	.5559	.08617	80		
23	.9483	.1470	52	.0064	.001	81		
24	.3426	.05310	53			82		
25	.9748	.1511	54			83		
26	.1581	.02451	55			84		
27	.4743	.07352	56			85	.5615	.08703
28	.05270	.008169	57					
29	.2108	.03268	58					

TABLE 5. - FINAL DESIGN OF SKIN (MEMBRANE) ELEMENTS BY FSD AND TFSD METHODS

Loads and Temperatures Given in Table 3.

Element Number	Thickness	
	cm	in
1	.002540	.0010
2	.006812	.002683
3	.002540	.0010
4	.03383	.01332
5	.03180	.01252
6	.002540	.0010
7	.02195	.008640
8	.005022	.001977
9	.02652	.01044
10	.03160	.01244

Final Mass 30.78 kg (67.80 lbm)

TABLE 7. - FINAL DESIGN OF TRUSS ELEMENTS OBTAINED BY TFSD AND FSD METHODS

Temperatures are 75 Percent of Those in Table 3.

Bar	Area		Bar	Area		Bar	Area	
	cm^2	in^2		cm^2	in^2		cm^2	in^2
1	.0064	.001	30	.0064	.001	59	.0064	.001
2			31			60		
3			32			61		
4			33			62	.3034	.04703
5	.04543	.007042	34			63	.0064	.001
6	.0064	.001	35			64		
7	.0064	.001	36			65		
8	.06813	.01056	37			66		
9	.0064	.001	38			67		
10	.0064	.001	39			68	.6065	.09401
11	.09845	.01526	40	1.315	.2038	69	.0064	.001
12	.0064	.001	41	.0064	.001	70		
13	.0064	.001	42			71		
14	.04543	.007042	43			72		
15	.0064	.001	44			73		
16	.0064	.001	45			74		
17	.01514	.002347	46			75		
18	.0064	.001	47			76		
19	.1324	.02053	48			77		
20	.08832	.01369	49			78		
21	.3532	.05475	50			79	.1033	.01601
22	.1324	.02053	51	.8593	.1332	80	.0064	.001
23	.9484	.1470	52	.0064	.001	81		
24	.3426	.05310	53			82		
25	.9748	.1511	54			83		
26	.1581	.02451	55			84		
27	.4743	.07352	56			85	.5634	.08733
28	.05271	.008169	57					
29	.2108	.03268	58					

TABLE 8. - FINAL DESIGN OF SKIN (MEMBRANE)

ELEMENTS BY TFSD AND FSD METHODS

Temperatures are 75 Percent of Those in Table 3.

Element Number	Thickness	
	cm	in
1	.00254	.001
2	.007313	.002879
3	.00254	.001
4	.03165	.01246
5	.03096	.01219
6	.00254	.001
7	.01639	.006452
8	.003325	.001309
9	.02670	.01051
10	.03193	.01257

Final Mass 29.10 kg (64.01 lbm)

TABLE 9. - FINAL DESIGN OF TRUSS ELEMENTS OBTAINED BY TFSD AND FSD METHODS

Temperatures One-half Values in Table 3.

Bar	Area		Bar	Area		Bar	Area	
	cm^2	in^2		cm^2	in^2		cm^2	in^2
1	.0064	.001	30	.0064	.001	59	.0064	.001
2			31			60		.001
3			32			61		.001
4			33			62		.05131
5	.04543	.007042	34			63		.001
6	.0064	.001	35			64		
7	.0064	.001	36			65		
8	.06813	.01056	37			66		
9	.0064	.001	38			67		
10	.0064	.001	39			68	.6793	.1050
11	.09845	.01526	40	1.231	.1908	69	.0064	.001
12	.0064	.001	41	.0064	.001	70		
13	.0064	.001	42			71		
14	.04563	.007042	43			72		
15	.0064	.001	44			73		
16	.0064	.001	45			74		
17	.01514	.002347	46			75		
18	.0064	.001	47			76		
19	.1324	.02053	48			77		
20	.08832	.01369	49			78		
21	.3532	.05475	50			79	.1994	.03091
22	.1324	.02053	51	1.101	.1707	80	.0064	.001
23	.9484	.1470	52	.0064	.001	81		
24	.3426	.05310	53			82		
25	.9748	.1511	54			83		
26	.1581	.02451	55			84		
27	.4743	.07352	56			85	.5802	.08993
28	.05270	.008169	57					
29	.2108	.03268	58					

TABLE 10. - FINAL DESIGN OF SKIN (MEMBRANE)

ELEMENTS BY TFSD AND FSD METHODS

Temperatures One-Half Values in Table 3.

Element Number	Thickness	
	cm	in
1	.002540	.001
2	.007714	.003137
3	.002540	.001
4	.02964	.01167
5	.03015	.01187
6	.002540	.001
7	.01218	.004796
8	.002540	.001
9	.02814	.01108
10	.03210	.01264

Final Mass 28.09 kg (61.80 lbm)

TABLE 11. - FINAL DESIGN OF TRUSS ELEMENTS OBTAINED BY TFSD AND FSD METHODS

Temperatures are One-fourth Values in Table 3.

Bar	Area cm^2	Area in^2	Bar	Area cm^2	Area in^2	Bar	Area cm^2	Area in^2
1	.0064	.001	30	.0064	.001	59	.0064	.001
2			31			60		
3			32			61		
4			33			62	.3494	.05415
5	.04543	.007042	34			63	.0064	.001
6	.0064	.001	35			64		
7	.0064	.001	36			65		
8	.06813	.01056	37			66		
9	.0064	.001	38			67		
10	.0064	.001	39			68	.7445	.1154
11	.09845	.01526	40	1.143	.1772	69	.0064	.001
12	.0064	.001	41	.0064	.001	70		
13	.0064	.001	42			71		
14	.04543	.007042	43			72		
15	.0064	.001	44			73		
16	.0064	.001	45			74		
17	.01514	.002347	46			75		
18	.0064	.001	47			76		
19	.1324	.02053	48			77		
20	.08832	.01369	49			78		
21	.3532	.05475	50			79	.2776	.04303
22	.1324	.02053	51	1.303	.2021	80	.0064	.001
23	.9484	.1470	52	.0064	.001	81		
24	.3426	.05310	53			82		
25	.9748	.1511	54			83		
26	.1581	.02451	55			84		
27	.4743	.07352	56			85	.6048	.09374
28	.05271	.008170	57					
29	.2108	.03268	58					

TABLE 12. - FINAL DESIGN OF SKIN (MEMBRANE)

ELEMENTS BY TFSD AND FSD METHODS

Temperatures One-Fourth Values in Table 3.

Element Number	Thickness	
	cm	in
1	.002540	.001
2	.008304	.003466
3	.002540	.001
4	.02776	.01093
5	.02941	.01158
6	.002540	.001
7	.009030	.003555
8	.002540	.001
9	.03007	.01184
10	.03216	.01266

Final Mass 27.57 kg (60.65 lbm)

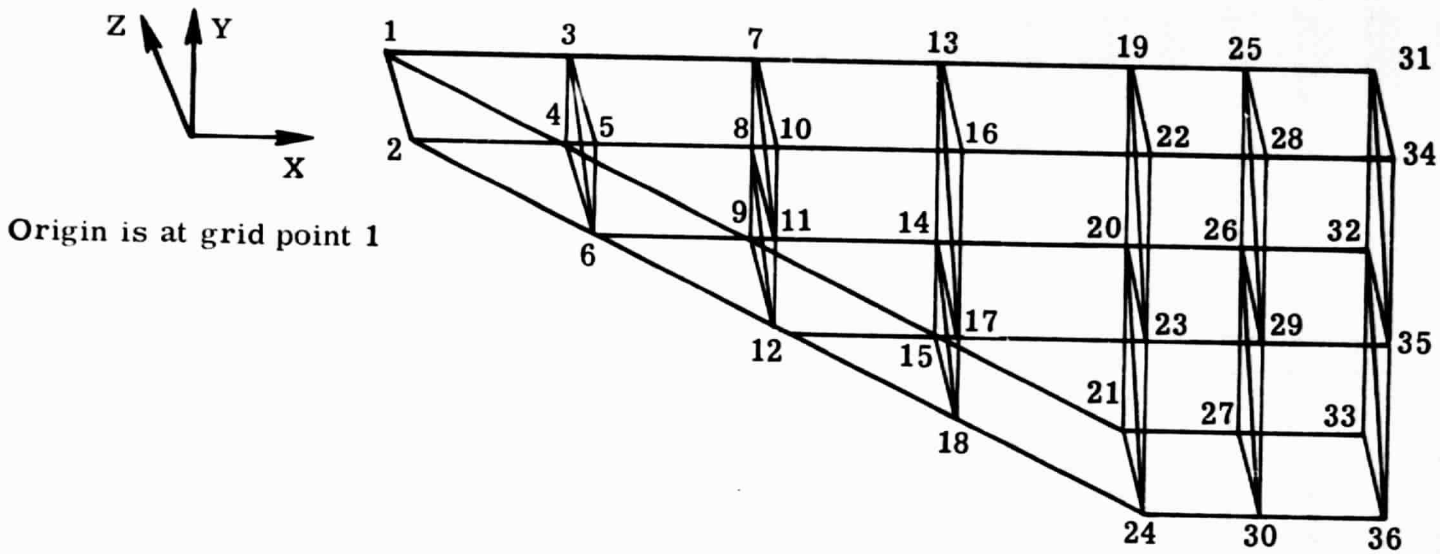

(a) Grid point locations and Truss elements

(b) Membrane elements

Figure 1.- Finite element model of built-up wing. $E = 200$ GPa (3×10^7 psi), $\rho = 8303$ kg/m^2 (0.3 lbm/in.^{7}), $\alpha = 12.0 \times 10^{-6}$/K ($6.5 \times 10^{-6}/^{o}$F), $\sigma_a = 0.97$ GPa (142 psi), $\nu = 0.3$.

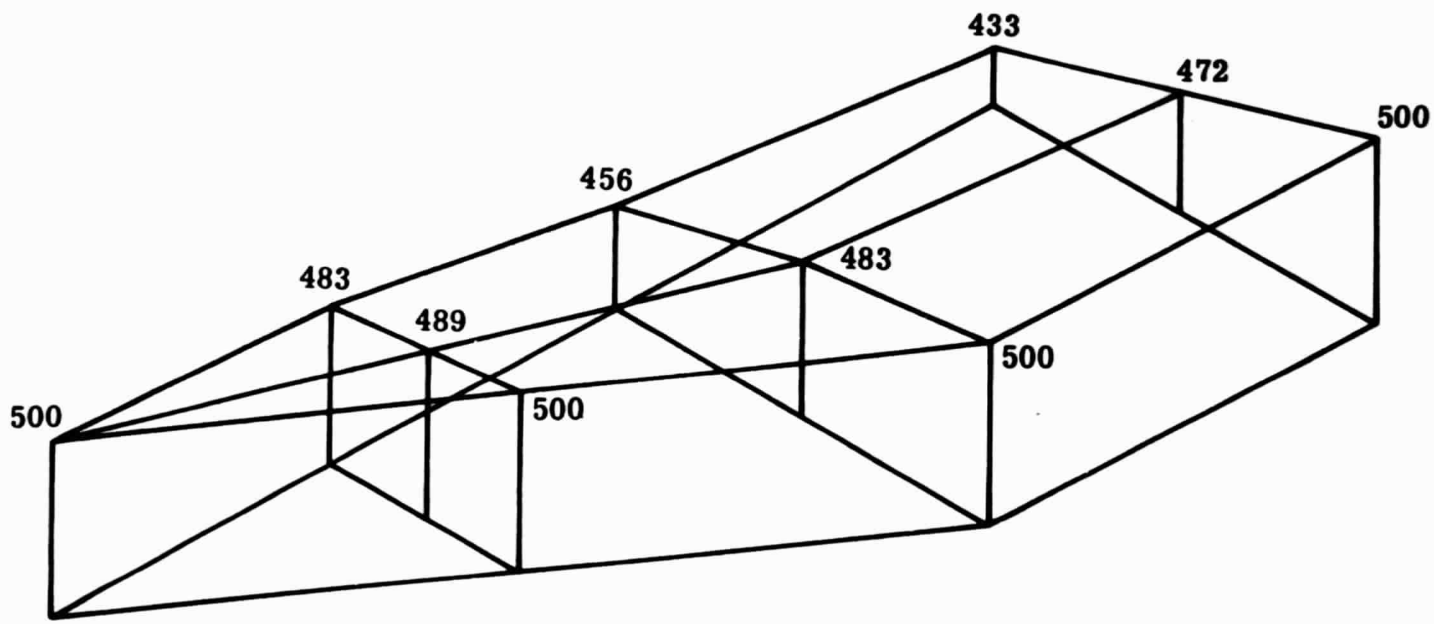

(a) Upper surface

Figure 2.- Temperature distribution on wing. (Values are in Kelvin)

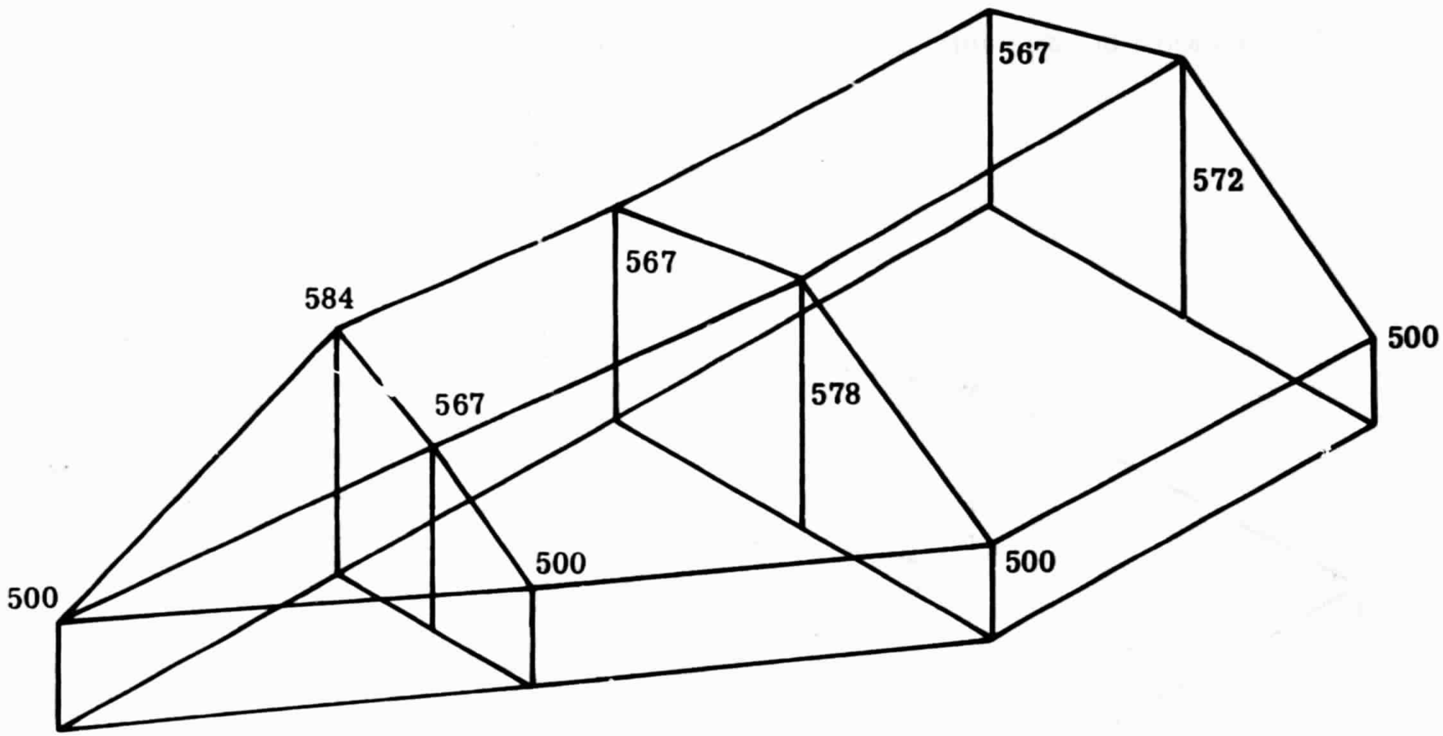

(b) Lower surface

Figure 2.- Concluded. (Values are in Kelvin)

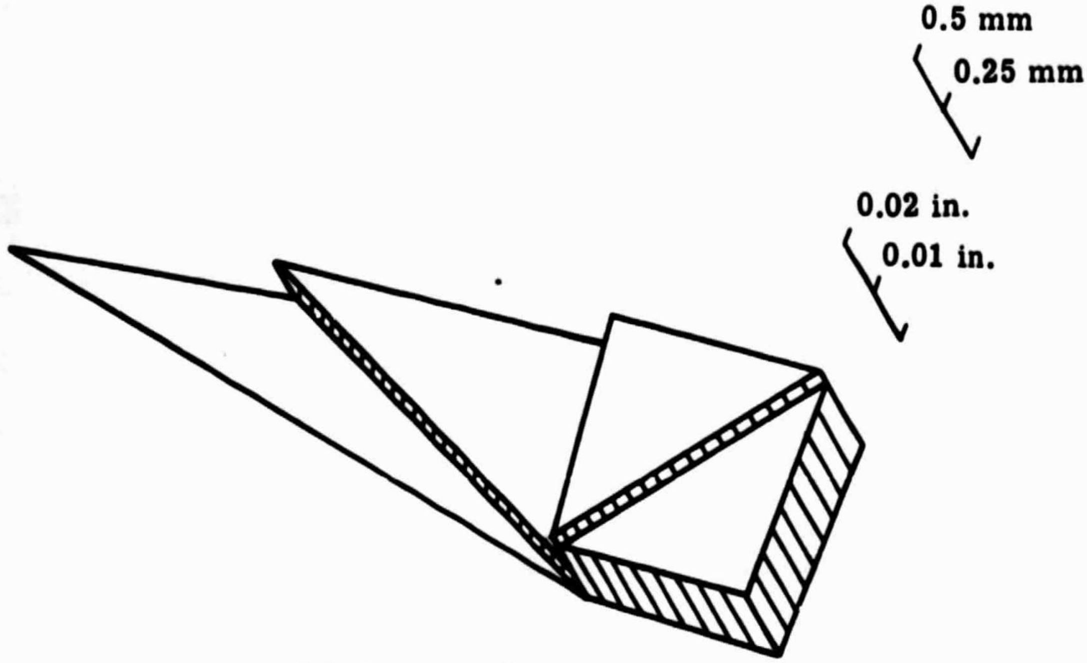

(a) Upper surface

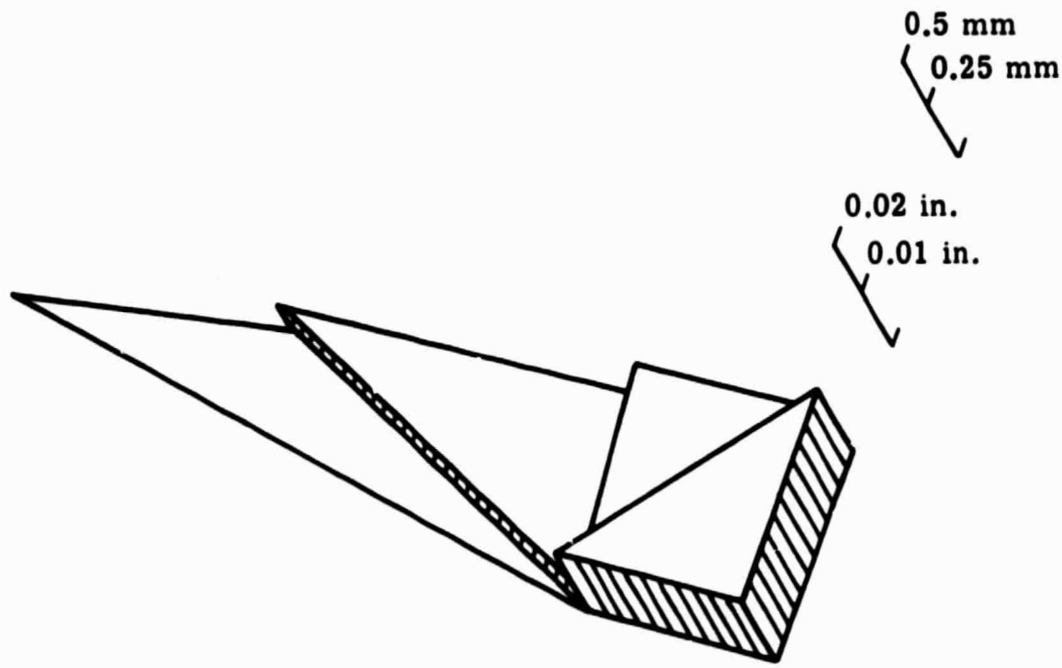

(b) Lower surface

Figure 3.- Distribution of membrane thickness in final design.

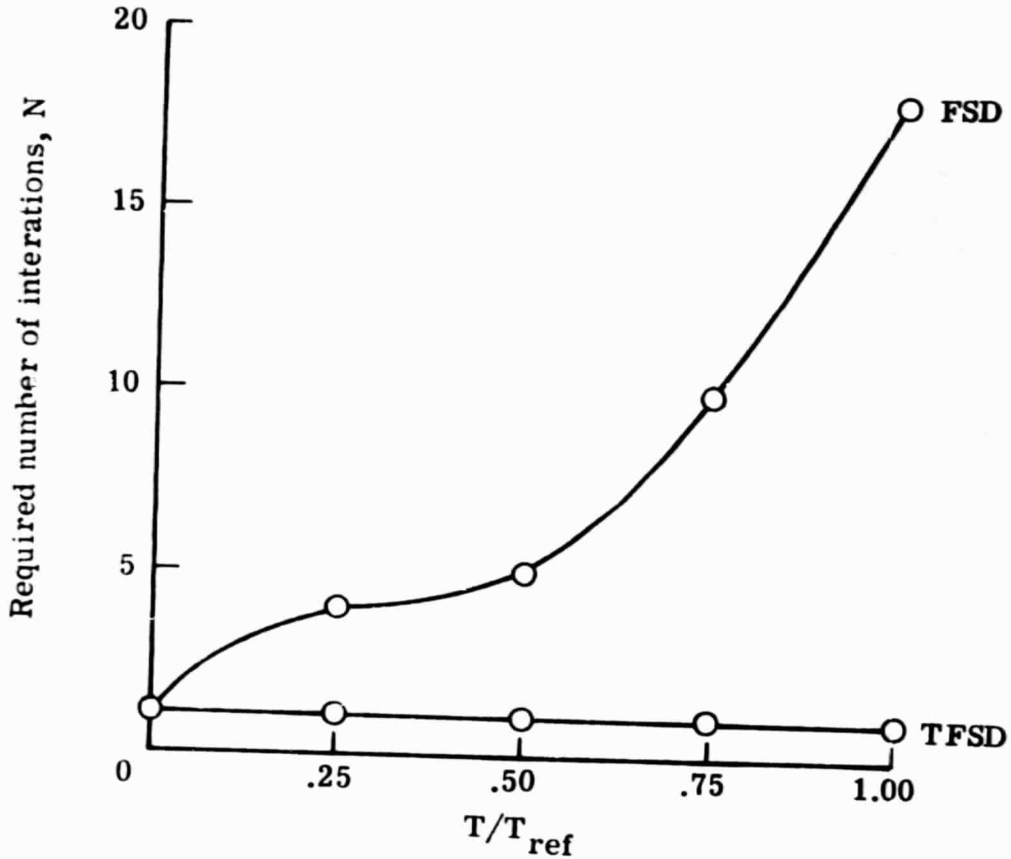

Figure 4.- Effect of thermal load level on convergence of FSD as compared to TFSD for sample problem. N = number of iterations for convergence within 5 percent of final mass.